

Zeitschrift: IABSE reports = Rapports AIPC = IVBH Berichte

Band: 49 (1986)

Artikel: Buckling of trapezoidally corrugated webs and panels

Autor: Bergfelt, Allan / Leiva-Aravena, Luis

DOI: <https://doi.org/10.5169/seals-38283>

Nutzungsbedingungen

Die ETH-Bibliothek ist die Anbieterin der digitalisierten Zeitschriften. Sie besitzt keine Urheberrechte an den Zeitschriften und ist nicht verantwortlich für deren Inhalte. Die Rechte liegen in der Regel bei den Herausgebern beziehungsweise den externen Rechteinhabern. [Siehe Rechtliche Hinweise.](#)

Conditions d'utilisation

L'ETH Library est le fournisseur des revues numérisées. Elle ne détient aucun droit d'auteur sur les revues et n'est pas responsable de leur contenu. En règle générale, les droits sont détenus par les éditeurs ou les détenteurs de droits externes. [Voir Informations légales.](#)

Terms of use

The ETH Library is the provider of the digitised journals. It does not own any copyrights to the journals and is not responsible for their content. The rights usually lie with the publishers or the external rights holders. [See Legal notice.](#)

Download PDF: 19.03.2025

ETH-Bibliothek Zürich, E-Periodica, <https://www.e-periodica.ch>

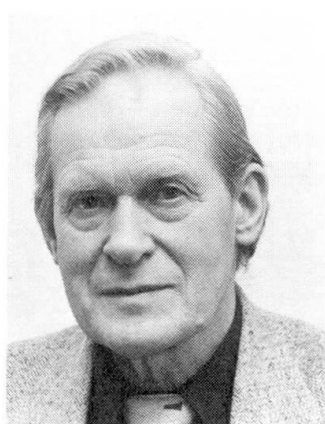
Buckling of Trapezoidally Corrugated Webs and Panels

Voilement de panneaux et d'âmes de poutres en tôle profilée
de forme trapézoïdale

Beulen von trapezförmig profilierten Stegen und Blechen

Allan BERGFELT

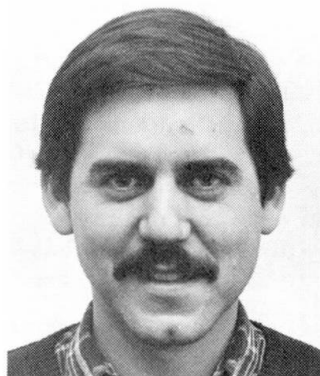
Professor Emeritus
Chalmers Univ. of Technology
Göteborg, Sweden



Allan Bergfelt, born 1915, graduated from Royal Inst. of Technology, Stockholm in 1937. After several years as a structural engineer, he was head of the design department, Gothenburg Harbour Authorities. Professor of Structural Engineering, Chalmers Univ. of Technology 1957 – 1981.

Luis LEIVA-ARAVENA

Research Assistant
Chalmers Univ. of Technology
Göteborg, Sweden



Luis Leiva-Aravena, born 1949, received his degree of Civ. Eng. (M.Sc.) at Chalmers Univ. of Technology in 1981. He is a research and teaching assistant at the Dep. of Structural Engineering, Div. of Steel and Timber Structures. His research work deals with buckling of thin-walled steel structures.

SUMMARY

Some test series on trapezoidally corrugated webs and panels are briefly presented. Local buckling seems to be governing for shear failure if the critical buckling stress is below or in the vicinity of the shear yield stress of the material. This seems to be valid for shear buckling for girder depths up to the region where global buckling calculated with common formulas may become critical. For combined axial and shear stress the best interaction curve seems to be a circle.

RÉSUMÉ

Des séries d'essais effectuées sur des panneaux et des âmes de poutres en tôle profilée de forme trapézoïdale sont brièvement présentées. La résistance ultime au cisaillement semble être gouvernée par un voilement local si la contrainte critique de voilement se trouve sous ou au voisinage de la contrainte limite de cisaillement du matériau. Cela semble valable au moins pour une hauteur de poutre qui se trouve en dessous de la limite de voilement global calculée avec les formules usuelles. Lorsque l'on combine contrainte normale et contrainte de cisaillement, la meilleure courbe d'interaction semble être l'arc de cercle.

ZUSAMMENFASSUNG

Einige Versuche mit trapezförmig profilierten Stegen und Blechen werden kurz beschrieben. Für die Schubbruchlast scheint das örtliche Beulen entscheidend zu sein, wenn die kritische Beulspannung unter oder in der Nähe der Schubfließspannung des Materials liegt. Dieses Verhalten scheint bei Trägerhöhen bis zu dem Bereich für das Schubbeulen gültig zu sein, bei dem das globale Beulen massgebend werden kann. Beim kombinierten Lastfall (Normal- und Schubspannung) wird eine kreisförmige Interaktionskurve vorgeschlagen.



1. INTRODUCTION

The type of welded steel girders with extremely thin, flat webs ($h/t \approx 220$) without any intermediate stiffeners, which were used in Sweden since the first years of the 1960's, met from the mid 60's a competition from girders with trapezoidally corrugated webs. These girders increased their part of the market and since the mid 70's they dominate the Swedish market for small and medium-span steel roofs.

The main reason for this situation is that it was possible to design the flat parts of the web with such a limited width, that no consideration to buckling of these parts had to be taken. Instead shear yield was governing for the dimensions ($\tau_{cr} \geq \tau_y$). The increase in allowable shear stress made it possible to use a thinner web and this compensated for the "longer" web plate, for the work of corrugating, and even for the loss of the possibility for the web to contribute to the bearing of bending moment of the girder. An extra advantage was that the specifications admitted one-sided welding, whilst flat webs were allowed with double-sided fillet welds only. The girders also had the advantage to be stiffer during handling than girders with flat webs.

As there was, of course, an interest to increase the span of the girders and thus their depth, there might be an influence of global buckling of the web and not only buckling of the individual plates between the folds. Research into this field was started in the first years of the 80's at the Division of Steel and Timber Structures at Chalmers University of Technology (CTH) as a part of a general research program within the field of thin-walled structures. Some preliminary reports on tests at CTH regarding this type of girders have been published [1], [2] and now some results are summarized here and supplemented with results from new tests.

Some of the new tests were mainly concerned with the problems of stiffening walls or "webs" in ships and in off-shore structures, where such walls may be designed as trapezoidally corrugated panels.

2. CALCULATIONS

2.1 Shear buckling

At the calculations the shear stress is presumed to be evenly distributed over the total depth of the web, $\tau = V/th \dots (1)$, see Fig.1b.

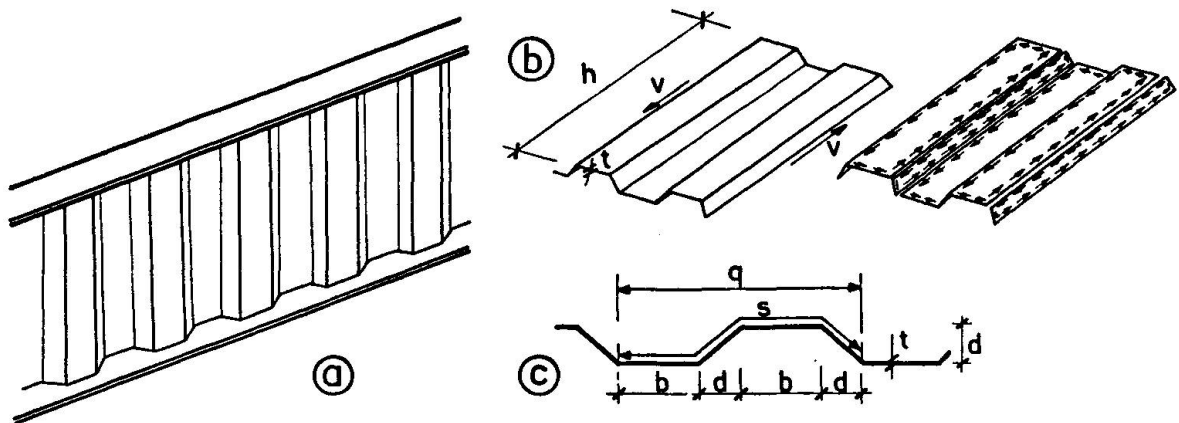


Fig. 1 Girder with corrugated web.

This stress must theoretically be smaller than the yield stress in shear τ_Y .

$$\tau \leq \tau_Y = \sigma_Y / \sqrt{3} = 0.577\sigma_Y \quad \dots(2)$$

The ideal (local) buckling of a plate of the web corresponds to

$$\tau_{cr} = \frac{k\pi^2 \cdot E}{12(1-\nu^2)(b/t)^2} \quad \dots(3)$$

Notations, see Fig.1c. Assuming ideal buckling and hinged edges (which gives a minimum value) you will have

$$\tau_{cr} / \sigma_Y = 4.83 / \lambda_w^2 \quad \text{where} \quad \lambda_w^2 = (b/t)^2 \cdot \sigma_Y / E \quad \dots(4)$$

However, there might be another type of buckling, too.

When the depth and length of the web are very large compared to the widths of single plates in the trapezoidal folded plate structure it might be possible that a long-wave buckle occurs over a larger portion of the web. This phenomenon is called "Global buckling".

Theoretical calculations, Ref. [3], [4], result in a formula for the critical shear force for global buckling N_{cr} (per unit length), that may be written:

$$N_{cr} = k_u \cdot (D_x \cdot D_y^3)^{1/4} / h^2, \quad \text{where} \quad D_x = \frac{q}{s} \cdot \frac{Et^3}{12} \quad \text{and} \quad D_y = \frac{EI_y}{q} \quad \dots(5a,b)$$

with $I_y = 2bt(d/2)^2 + 2\sqrt{2} \cdot d^3t/12$ for a symmetrical trapezoidal shape with 45° folds, c.f. Fig.1c.

The results of a calculation of k_u , given in Ref. [3], is $k_u = 32.4$ for hinged edges and 60.4 for fixed edges. (In most of the formulas given E is used instead of $E/(1-\nu^2)$ even for the plate stiffness D_x .) For a panel with fixed edges the critical shear stress for global buckling thus may be written

$$\tau_g = N_{cr} / t = 60.4 \cdot (D_x \cdot D_y^3)^{1/4} / h^2 t \quad \dots(6)$$

or with D_x and D_y inserted:

$$\tau_g = N_{cr} / t = \frac{60.4}{\sqrt[4]{96}} \underbrace{\left[\frac{q}{s} \cdot \left(\frac{\sqrt{2}}{3} + \frac{b}{d} \right)^3 \cdot \left(\frac{d}{q} \right)^3 \right]^{1/4}}_{p_g} \cdot \frac{d\sqrt{td}}{h^2} \cdot E \quad \dots(6b)$$

Here a factor p_g , "the global buckling product", is defined in formula (6b) for a web shape like Fig.1c, which is intended to make it easier to directly see the influence of the geometry of the web as p_g varies rather little. It was $p_g = 0.52$ and 0.54 respectively for the ideal shape of the tested webs and $p_g = 0.48-0.53$ for various imperfect waves.

2.2 Combined axial and shear stress

In a girder with a transversally corrugated web the normal stresses due to bending are produced mainly in the flanges. Any "horizontal" normal stress σ_x is produced in the web, only locally and in the vicinity of the flanges. A "vertical" stress σ_y may be introduced locally at the supports and at the points of loading.



In bulkheads or "webs" used as stiffening panels in ship structures and offshore structures there may, however, occur large forces introduced in the direction of the folds in a trapezoidally corrugated panel, all over the length of the panel.

The critical buckling load for these stresses σ_y ought to be σ_{cr}^y for the folded web seen as a column and σ_{cr}^{yp} for the individual plates

$$\sigma_{cr}^y = c \cdot \frac{\pi^2 EI_y}{A \cdot h^2} ; \quad \sigma_{cr}^{yp} = \frac{k\pi^2 E}{12(1-\nu^2)(b/t)^2} \quad \dots(7a,b)$$

With a general shape of the interaction formula you may write

$$\left(\frac{\sigma_y}{\sigma_{cr}^y}\right)^2 + \left(\frac{\tau}{\tau_{cr}}\right)^2 \leq 1 \quad \dots(8)$$

3. TESTS

3.1 Shear buckling, local and global

In order to obtain optimal economy of trapezoidally corrugated girder webs it is often convenient to choose the geometry of the corrugation in such a way that local buckling shear stress (eq.3) will be about the same as shear yield stress ($\tau_{cr} \approx \tau_y$). In Sweden such girder webs with standardized geometry have been used since the 1960's ($b = 140$ mm, $d = 50$ mm). In order to find the limit to which it is possible to increase the girder depth without making global buckling (eq.5a,b) the governing mode, i.e. making local buckling occur first, some test series have been performed, which were published in ref. [2].

Now a further test series has been performed and the former survey figure is supplemented with the new results. The new figure, Fig.2, is drawn in a way, which is thought to be more illustrative (and at the same time some misprints in the old material are corrected). At the horizontal axis the girder depth is represented as h/h^* , where h^* is the depth at which the theoretical critical global buckling stress τ_g (from eq.6) will coincide with the shear yield stress τ_y . Thus the formula for h^* is

$$h^* = \left[60.4 \cdot (D_x \cdot D_y^3)^{1/4} / \tau_y \cdot t \right]^{1/2} \quad \dots(9)$$

The calculated values of h^* for the different test girders are listed in Fig.2. The intention with the web geometry chosen in the specifications was to obtain $\tau_{cr} \approx \tau_y$. As this was not exactly the case for the test girders the ratios τ_d/τ_y are marked out in the diagram of Fig.2, too. Here τ_d is chosen to represent τ_{cr} , as a reduction is necessary when the buckling values are near the yield values. $\tau_d/\tau_y = \sqrt{3} \cdot 1.4 \frac{t}{b} \sqrt{E/\sigma_y}$ following the Swedish specifications for this region (when a value > 1 is obtained, the value 1.0 is denoted).

It is seen that even for the deepest of the girders tested local buckling was the phenomenon that started the buckling. Any obvious interaction between local and global buckling is difficult to observe even for girders with depth near to those where global buckling ought to dominate.

Any decrease of the load carrying capacity in the vicinity of the region where the curve for global buckling in Fig.2 passes under the level of τ_y , which was indicated by the first tests, c.f. ref. [2], thus is not confirmed. In connection to this it is to be observed that the high value of 60.4 corresponding to fixed edges is chosen for the constant k_u in the formula, eq. 5a and 6. With the value 32.4 for

hinged edges, the failure loads at the tests very clearly surpass any such "theoretical" global buckling.

When the deformations were driven further, however, the local buckling developed into "zonal" buckling and then into global buckling. The deformations ended into a very marked tension field as described in ref. [2].

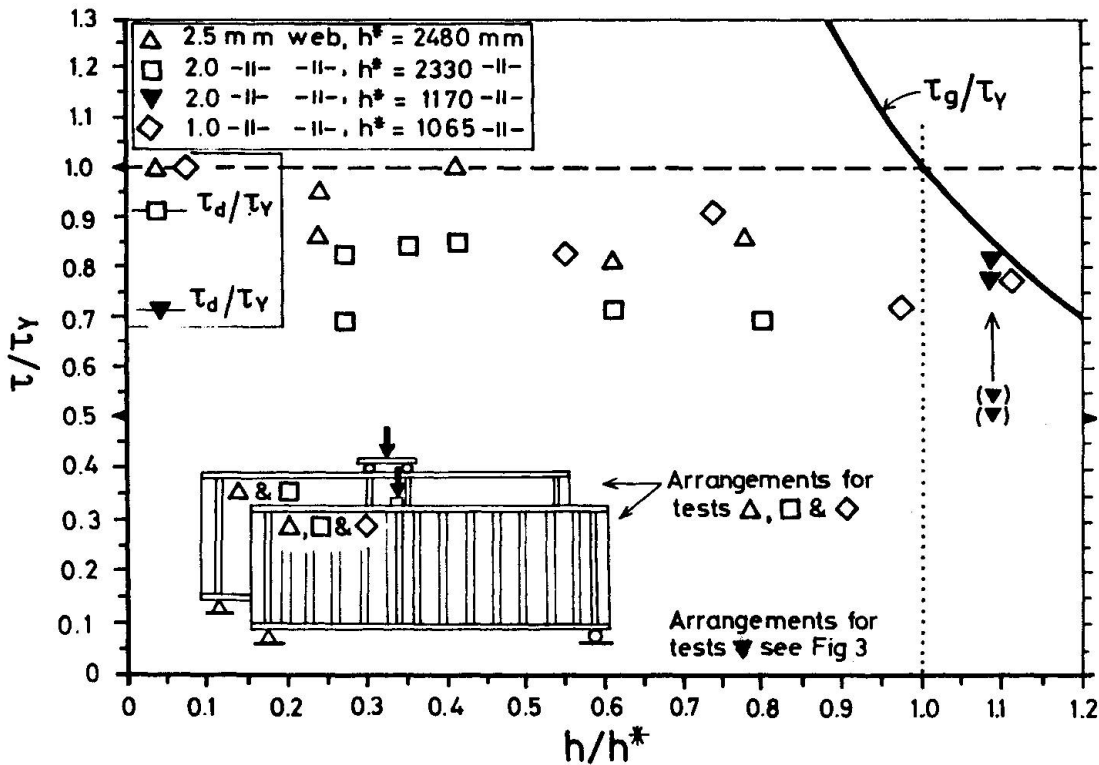


Fig. 2 Shear stress at buckling. Survey of test results.

3.2. Combined shear and normal buckling

3.2.1 General arrangement

The test series of elements under combined shear and normal stresses were made with elements of another geometry than that of the elements for girder tests. The reason was the intention to choose a geometry that could be seen as a model of what was thought to be a typical design for "walls" and panels in shipbuilding and off-shore structures.

The test arrangement was also different from that of the girders, and the loading giving vertical stresses were distributed all along the upper flange, while the horizontal force was introduced at one end of the upper flange, see Fig.3. The lower flange was vertically supported all along, but the horizontal reactions were taken by welding along about half the length of the flange. It was at first intended to take the horizontal reaction concentrated locally at the lower flange vertically under the horizontal load, but the welds then ought to be very large, and so the welding was spread out.

A weld all along the lower flange was not seen as necessary as the shear stress was relatively small. The reason of placing the weld at the same end as the horizontal force was, of course, to prevent lifting at this end at small vertical forces.

The test results of a pure shear loading is introduced in Fig.2. However, the flat



parts of the wall panel had a largest width of 171 mm for a 2 mm thick plate and thus local buckling was dominating. In order to make a comparison with the webs in Fig.2 directly possible, the test results are enlarged in proportion $(171/140)^2$. The original results are given, too, but these points are put within brackets.

All the results for the walls, both at combined loading, at purely shear loading and at purely vertical loading are collected into Fig.6.

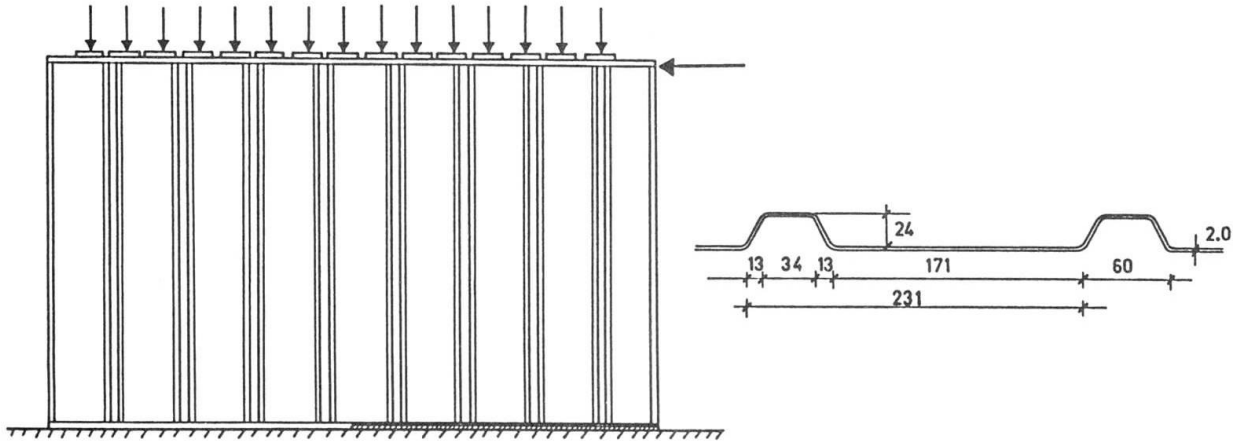


Fig. 3 Arrangement of panel testing. Section of the panel.
(Panel $h = 1270$ mm, $l = 1995$ mm.)

3.2.2 Testing performance

The vertical load resulting in buckling is to be calculated as for a column, and thus is obtained from eq.(7a). The global buckling load is calculated from eq.(6). As the geometry is unsymmetrical it is not possible to utilize the simplified eq.(6b).

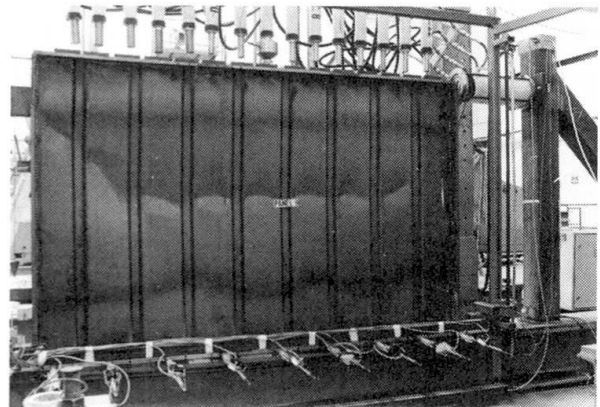
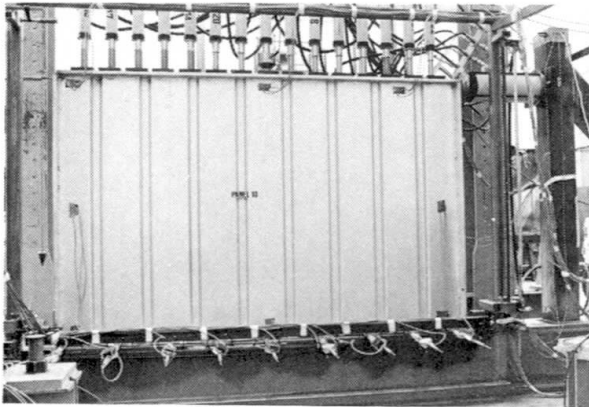
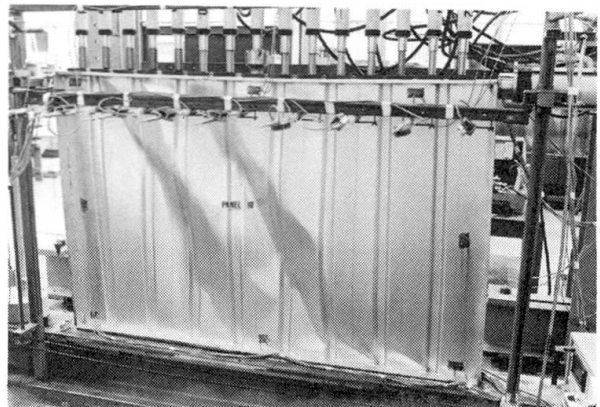


Fig. 4 Panel testing, arrangement.

Fig. 5 Buckling pattern after testing. Panel P9 and P10 resp.



The first experiments checked the two extreme points, that is buckling at pure vertical load and buckling at pure horizontal (shear) load. Further experiments were performed with such loading levels that the total vertical loading span was divided into six parts. The vertical load was introduced by 15 hydraulic jacks, coupled to give equal force.

Quite as for the girder tests the strains (stresses) were measured at several points of the web. The detailed result of these measures will be given in the detailed reports.

3.2.3 Test results

Two typical buckling modes at large deformations are illustrated in Fig.5. All buckling test results are given in Table 1 and are illustrated in Fig.6. The vertical stress σ_y in Table 1 is calculated as the sum P of all the vertical jack forces divided by the total section area. As there were vertical stiffeners at the ends taking part of the load, this means that the σ_y given are true only at the middle part of the web. The shear stress τ is calculated by dividing the force H of the horizontal jack by the projected length of the web times the web thickness. Even here some deviation may occur at the ends. A detailed calculation will be given in connection with the discussion of the strain gauges results.

The σ_{cr}^y from eq. (7a) calculated with $c = 1.8$ is 179 N/mm^2 (the coeff. c is calculated with consideration to end conditions and imperfections, by using the Swedish specifications). The σ_{cr}^P from eq. (7b) is 101 N/mm^2 with $k = 4$, τ_{cr} from eq.(3) is 135 N/mm^2 with $k = 5.34$ and σ_y for the material was 191 N/mm^2 . In Fig.6 the experimental values $\sigma_{cr}^{exp} = 156 \text{ N/mm}^2$ and $\tau_{cr}^{exp} = 101 \text{ N/mm}^2$ are used in eq.(8) for the curve of comparison. Even this choice will be discussed in connection to the strain gauges results.

It is seen that eq.(8) gives a fair picture of the interaction.

Table 1. Panel tests.

Test No	P_{\max} kN	H_{\max} kN	$\sigma_{\max}/\sigma_{cr}^{exp}$	$\tau_{\max}/\tau_{cr}^{exp}$
P4	0	388	0	0,97
P5	0	409	0	1,02
P8	195,0	430	0,28	1,08
P10	225,0	334	0,33	0,84
P6	375,0	303	0,55	0,76
P7	535,5	252	0,78	0,63
P9	592,5	166	0,86	0,42
P3	672,0	0	0,98	0
P2	700,5	0	1,02	0
P1	816,0	0	1,19	0

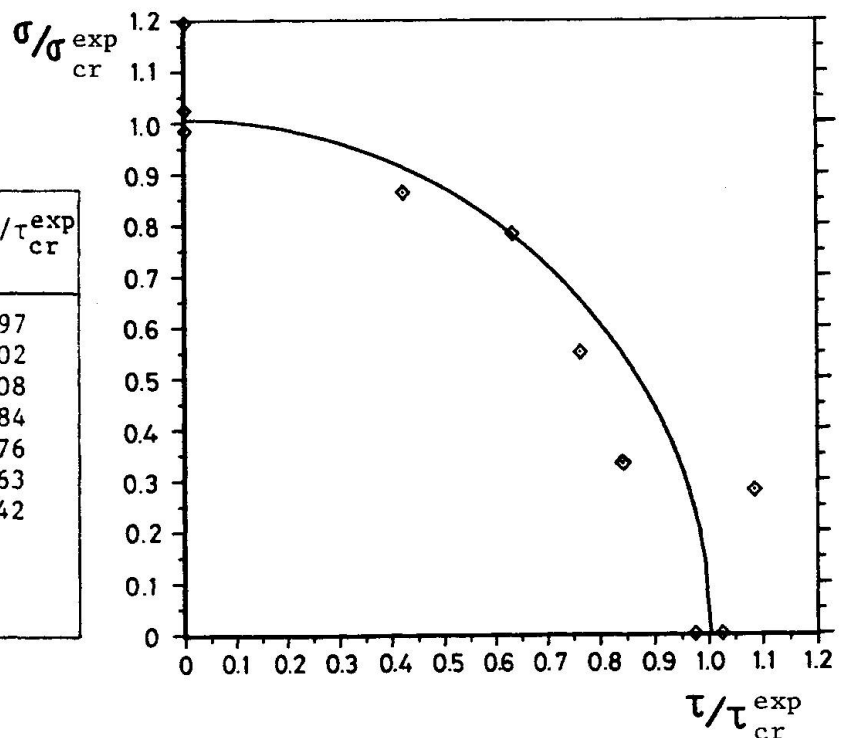


Fig. 6 Buckling stresses at combined axial load and shear load.



4. CONCLUSIONS

Any influence of global buckling on the shear buckling of the web of girders with the tested geometry seems very small. It seems necessary to extend the testing to deeper girders and also to girders with larger length-to-depth ratio in order to confirm any influence of global buckling.

The interaction curve for σ_y and τ followed principally the shape given by eq.(8).

REFERENCES

1. LEIVA L., *Skivbuckling hos plåtbalkar med trapetsprofilerat liv*. Delrapport 1. CTH, Stål-och Träbyggnad. Publ. S 83:1, Göteborg 1983. (In Swedish.)
2. BERGFELT A., EDLUND B., LEIVA L., *Trapezoidally corrugated girder webs*. Schweizer Ingenieur und Architect 1-2/85 s.22.
3. EASLEY J.T., *Buckling Formulas for Corrugated Metal Shear Diaphragms*. Journal of the Structural Div. ASCE, 1975, No ST 7, p.1403-1417.
4. PETERSON J.M., CARD M.F., *Investigation of the Buckling Strength of Corrugated Webs in Shear*. NASA Technical Note D-424. Washington 1960.

APPENDIX

TABLE

Test results plotted in Fig. 2. This is essentially table 1 in ref. [2] with some misprints corrected.

Girder	t mm	h mm	σ_y N/mm ²	λ_w	τ_d N/mm ²	R _{max} kN	τ_{max}^{exp} N/mm ²
L1A	1.94	1000	292	2.69	152	280	140
L1B	2.59	1000	335	2.16	217	502	201
L2A	1.94	1500	282	2.64	150	337	112
L2B	2.54	1500	317	2.14	207	564	150
L3A	2.01	2000	280	2.54	154	450	113
L3B	2.53	2000	300	2.09	201	775	155
B1	2.10	600	341	2.65	181	208	165
B4	2.11	600	363	2.72	187	183	145
B4b	2.11	600	363	2.72	187	217	171
B3	2.62	600	317	2.04	212	246	156
B2	2.62	600	315	2.04	211	273	174
M101	0.99	600	189	2.10	127	53	89
M102	0.99	800	190	2.11	126	79	99
M103	0.95	1000	213	2.23	134	84	85
M104	0.99	1200	189	2.10	127	101	88